

Yu.G. Chabak^{1,2}, M.A. Golinskyi¹, V.G. Efremenko^{1,2*}, H. Halfa³, V.I. Zurnadzhy^{1,2},
B.V. Efremenko¹, E.V. Tsvetkova¹, A.V. Dzherenova¹

Ti-rich carboborides in the multi-component high-boron alloy: morphology and elemental distribution

¹Pryazovskyi State Technical University, Dnipro, Ukraine, vgefremenko@gmail.com

²Institute of Materials Research of Slovak Academy of Sciences, Kosice, Slovakia

³Central Metallurgical Research and Development Institute, Eltebbin, Helwan, Cairo, Egypt

In the article, the characterization of the morphology, chemical composition, and elemental distribution in the Ti-based carboboride M(C,B) in (wt.%) Fe-0.72C-2.75B-5.05W-5.57Mo-10.35Cr-2.60Ti multi-component alloy is fulfilled. The study was performed using optical microscopy, SEM, TEM, and energy-dispersive X-ray spectroscopy. It was found that the carboboride M(C,B) is present in the structure in the form of the equiaxed polygonal particles of a 0.5-7.3 μm mean size. The particles are divided into “duplex” and “uniform” ones. The duplex particles consists of the Ti-rich (75 wt. % Ti) “core” (Ti(C,B)) and the Ti-depleted (47.3 wt. % Ti) “shell” ((Ti,W,Mo,V)(C,B)). The uniform particles are characterized by an even distribution of the elements having a chemical composition close to the “shell”. The ratio of B:C (at. %) is 1:2.5, 1:3.3, and 1:3.2 for the “core”, “shell” and the uniform particle respectively. The chemical formulas of the duplex/uniform M(C,B) inclusions and the mechanism of their formation are proposed.

Keywords: multi-component cast iron, microstructure, EDS, Ti-rich carboboride, duplex inclusion.

Received 19 August 2023; Accepted 22 November 2023.

Introduction

Titanium carbide TiC and titanium boride TiB₂ are important structural components of various materials of tribological applications (cast irons, tool alloys, composites, etc) [1-3]. Their main advantage is a high hardness (2500-3200 HV [4]) exceeding the hardness of the most abrasive particles thus effectively improving the abrasive wear resistance of different alloys (high-Cr cast iron [5], CoCrMo biomedical alloy [6], hardfacing layers [7], coating [8], composites [9], etc.). TiC and TiB₂ have advanced thermal stability similar to the refractory ceramic [10]; also, they crystallize first from the melt refining the structure of cast alloys due to the nucleation effect [11-14]. Wu et al. [12] found that adding 1.5 wt. % Ti led to a 2.5 times decrease in the equivalent diameter of coarse primary carbides M₇C₃ in a 4 wt.%C-20wt.%Cr hyper-eutectic cast iron. The same effect was reported by Zhang et al. [13] who revealed the strong nucleation effect

of TiC–NbC core-shell carbide in a 3.7wt.%C-25wt.% Cr cast iron due to lower mismatch with M₇C₃ meaning stronger nucleation efficiency. Bedolla-Jacuinde et al. reported [14] that introducing 2 wt.% Ti into the 2.5wt.%C-15wt.%Cr-3wt.%Mo resulted in a decrease in the SDAS (the secondary dendrites arm spacing) from 25 μm to 18 μm . In the high-boron alloys, the addition of titanium reduces brittleness by replacing the eutectic Fe₂B-based network with uniformly distributed equiaxed particles of titanium diboride TiB₂ [15, 16].

When added to Fe-C-B alloys, titanium binds with carbon rather than with boron. According to [17], alloying of high-boron high-speed steel by 0.2-0.55 wt.% Ti resulted in the formation of TiC carbide; at the same time, titanium borides were not found despite the presence of 2 wt.% B in the alloy. Under higher Ti content and higher C/B ratio, the formation of Ti-based borocarbide (such as TMB₂C, where TM includes Ti, V, Cr, Mn, and Fe [18]) is possible. Due to a very high affinity for carbon, titanium

prevails in competition with other elements, forming carbide with a high content of titanium and a minimum presence of other elements [19]. However, when other carbide-forming elements (W, Mo, V) are added in the higher concentrations, they may participate in the formation of TiC leading to partial substitution of titanium in carbide's lattice. This case refers to the "hybrid" high-boron multi-component alloys [20-22] in which the complex-alloyed Ti-based carboboride $M(C,B)$ was found. This compound is the focus of the present work regarding its structural features, chemical composition, and elemental heterogeneity.

I. Methods

The experimental material was a hybrid high-boron multi-component alloy studied in [21, 22]. The alloy was fabricated by conventional casting into sand molds according to the procedure detailed in [21] with a chemical composition of: 0.72 wt.% C; 2.75 wt.% B; 0.90 wt.% Mn; 1.10 wt.% Si; 10.35 wt.% Cr, 5.05 wt.% W, 5.57 wt.% Mo, 2.60 wt.% Ti, Fe - balance. The specimens were cut from the cast billet and then polished and etched by 4%-Nital reagent. The microstructure was observed using the optical microscope (OM) Olympus GX71, scanning electron microscopy (SEM) JEOL JSM-7000F, and transmission electron microscope JEOL JEM-2100F/CESCOR. The elemental composition was determined by energy-dispersive X-ray spectroscopy (EDS) using the detector INCAx-sight (Oxford

Instruments). The average of 4-6 measurements performed on the same structure/phase constituents was taken as a phase chemical composition.

II. Results and Discussion

The comprehensive experimental study and thermodynamic analysis of the structure formation in the alloy studied were performed in our previous works [21-23]. As seen from Figure 1a, the alloy has a heterogeneous structure consisting of different phase constituents, specifically [21, 22]: (a) the coarse prismatic-shaped inclusions (primary boron-carbide $M_2(B,C)_5$), (b) elongated eutectic plates of boron-carbide $M_2(B,C)_5$ and carboboride $M_7(C,B)_3$, and (c) the dark equiaxed dispersed inclusions shown by the arrows in Fig.1a (Ti-rich carboboride $M(C,B)$) (for all phases M includes most of all carbide-forming elements present in the alloy).

The magnified images of the Ti-based carboborides are shown in Figs. 1b-1d. The volume fraction of these inclusions was measured previously as 7.3 vol. % [21]. They have a near-square polygonal faceted shape with a mean side of 0.5-7.3 μm ($4.22 \pm 0.48 \mu\text{m}$ on average). The inclusions mostly were spread separately; with that, the occasional particle-conglomerates were also seen with sizes up to 35 μm in length and 25 μm in width (Fig. 1b). The major fraction of the particles have a duplex structure with a clearly distinguished "core"/"shell" pattern: as seen in Fig. 1b, in the optical microscope, the "core" is yellow-colored while the "shell" is grey-colored. The rest of the

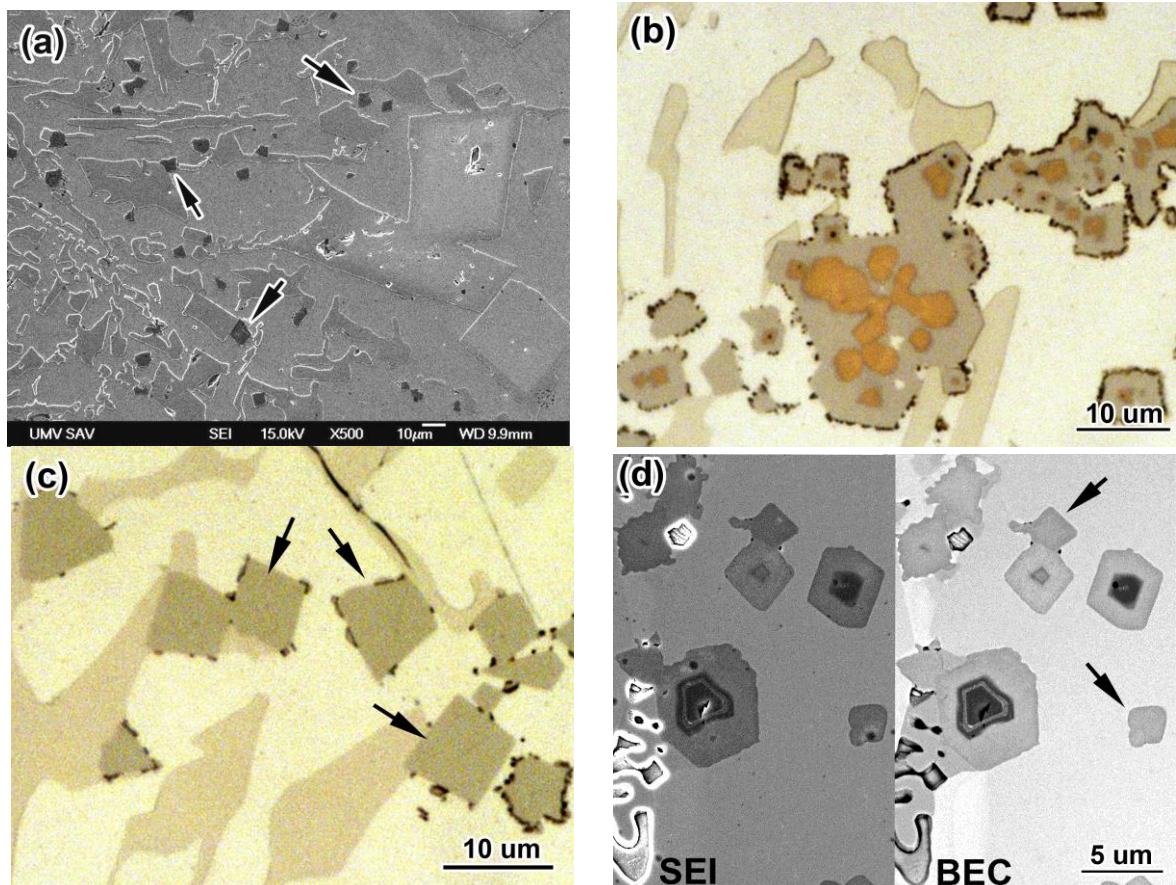


Fig.1. Microstructure of the experimental alloy: (a) the total view, (b) the duplex $M(C,B)$, (c) the uniform $M(C,B)$, (d) the duplex and uniform particles (a – SEM/SEI image, b, c – OM images, d – SEM/SEI/BEC image).

particles have a uniform grey-colored morphology (denoted by the arrows in Figs. 1c and 1d). In the SEM/SEI (Secondary Electron) images the “core” is differentiated as the dark-contrast polygonal area with clearly delineated boundaries (Fig. 1d). The shape of the “core” roughly corresponds to the shape of the inclusion. Occasionally, the “core” features a dendrite-like shape (Fig. 1b) which is characteristic of the larger particles. On SEM/BEC (Back-Scattered Electron Composition) images (Fig. 1d, the right side), the core has a dark color indicating its enrichment with elements of low atomic number which are most likely boron ($Z_B=5$), carbon ($Z_C=6$), and titanium ($Z_{Ti}=22$). The duplex and uniform inclusions have the same size distribution.

The elemental inhomogeneity of the duplex M(C,B) inclusions was more precisely studied using the EDS analysis. Fig. 2 presents the profiles of the elements’ distribution across the inclusions. In the duplex particle (Fig. 2a), the titanium profile demonstrates a high content of this element (as-compared to the matrix) with an additional pronounced increase in Ti content corresponding to the “core”. Both profiles of carbon and boron have a significant drop attributed to the “core”, while carbon concentration, in general, is higher as compared with boron. The same profile shape (with a decrease in the “core” to the matrix level) is characteristic of W and Mo profiles (Fig. 2b). The distribution of vanadium is more even relatively W and Mo, with only a slight decrease in the “core”. Iron is almost completely absent in the inclusion. Figs. 2a and 2b reveal that the duplex inclusion is a complex-alloyed Ti-rich carboboride where Ti is mostly concentrated in the “core” while the

other elements (C, B, W, Mo) are mainly gathered in the “shell”. This results in the dark BEC-contrast of the “core”, since the atomic number of Ti is much lower than that of other carbide-forming elements.

The uniform inclusion (Figs. 2c and 2d), as in the case above, performs an increased (relative to the matrix) contents of C, B, Ti, W, Mo, and V. The distinctive feature of the uniform particle is the roughly level distribution of the elements within it. The only noticeable exception is a slight increase in the concentration of molybdenum at a reduced content of titanium in the peripheral areas of the inclusion (marked by arrows in Figs. 2c and 2d).

The quantitative data on the “core”/“shell” chemical compositions was obtained by the point EDS analysis. As follows from Fig. 3, the results of the measurements are in full accordance with the elements profiles (Fig. 2). The average concentration of titanium in the “core” (75.6 wt.%) is by 32 wt. % higher as compared to the “shell”. Accordingly, the total amount of carbon and boron in the “core” (16 wt. %) is by 10.8 wt.% lower than that of the “shell”. Taking into account the residual amounts of other elements (less than 9 wt. % in total), the atomic concentration of titanium in the “core” is 83.7 at.% which is close to the stoichiometric atomic concentration of titanium in the TiC carbide (80 wt.%). Thus, the “core” can be considered as a TiC where carbon is partially replaced with boron (their atomic concentrations in the inclusion are 9.7 at.% and 5.3 at. % respectively). In the “shell”, titanium is still a major element but the amounts of other elements (W, V, Mo, Fe) are much bigger than in the “core” reaching 25.9 wt.% in total. (Among them tungsten is a main contributor performing a 10 wt.%)

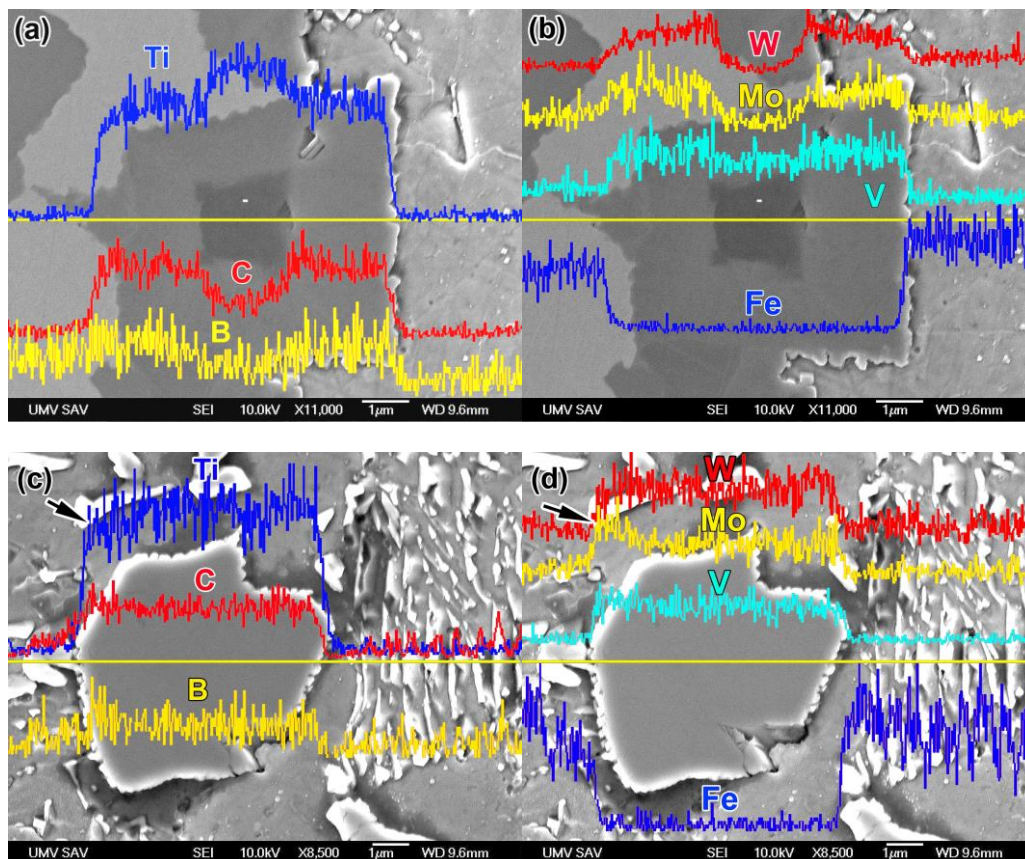


Fig. 2. The profiles of the elements (a, c) C, B, Ti, and (b, d) W, Mo, V, Fe across (a, b) the duplex M(C,B) particle and (c, d) the uniform M(C,B) particle.

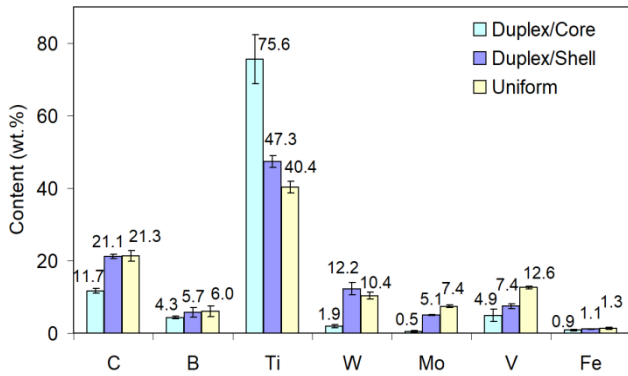


Fig. 3. The chemical compositions of the duplex and the uniform Ti-rich carboborides M(C,B).

increment in content as compared to the “core”). Accordingly, the atomic content of Ti in the “shell” is only 64.9 at.% while the carbon and boron contents are increased to 21.7 at.% and 8.7 at.% respectively. The difference in the chemical composition between the “core” and the “shell” is illustrated by the EDS spectra shown in Fig. 4. Based on the elemental compositions, the formulas for the “core” and the “shell” can be presented as $(\text{Ti}_{0.92}\text{V}_{0.06}\text{W}_{0.01}\text{Fe}_{0.01})(\text{C}_{0.71}\text{B}_{0.29})$ and $(\text{Ti}_{0.78}\text{V}_{0.11}\text{W}_{0.05}\text{Mo}_{0.04}\text{Fe}_{0.02})(\text{C}_{0.77}\text{B}_{0.23})$, respectively.

As follows from Fig.3, the chemical composition of the uniform Ti-rich particles is rather close to the “shell” with a negligible difference in the contents of C, B, W, and Mo. More notable differences refer to Ti (decrease by 6.9 wt.%) and V (increase by 5.2 wt.%). The atomic concentration of Ti is 59.4 at.% which is even lower than that of the “shell”. This is also confirmed by a change in the ratio of the intensity of the Ti and (W, V, Mo) energy peaks presented in Fig. 4c. The formula of the uniform inclusion is $(\text{Ti}_{0.67}\text{V}_{0.20}\text{Mo}_{0.06}\text{W}_{0.05}\text{Fe}_{0.02})(\text{C}_{0.76}\text{B}_{0.24})$. The ratio of B:C (at. %) is 1:2.5, 1:3.3, and 1:3.2 for the “core”, “shell” and the uniform particle, respectively, thus Ti-depleted inclusions contain more carbon and less boron as compared with the Ti-rich “core”.

The formation of two morphologically different Ti-based compounds is presumably resulted from the conjoint introduction of the alloying elements which form the carbide/boride under the solidification in a high-temperature area. Figure 5a presents the “Thermo-Calc”-calculated pseudo-binary phase diagram “M – Boron” (M is the chemical composition of the alloy, excluding B) adopted from [23] where the experimental alloy is denoted by the red dotted line. According to the diagram, in the present alloy, a tungsten boride WB is the first which starts solidifying at 1472°C. At 1460°C, TiC carbide starts crystallizing. Further, WB and TiC solidify together in a

wide temperature range of 1460-1126 °C, where the lower Gibbs energy corresponds to TiC (Fig. 5b), meaning its leading role in structure formation.

It can be suggested that under solidification, the first nuclei of TiC appeared in those Ti-rich melt pools where the Ti content is sufficient to bind with carbon in the stoichiometric proportion. According to Figs. 5a and 5b, titanium boride TiB_2 does not appear at temperatures less than 1000 °C. However, in the interval of 978...475°C [23] it is TiB_2 that has the lowest Gibbs energy reflecting the high potential of boron for binding with Ti. As follows from the EDS results, this potential showed itself even at higher temperatures when boron competed with carbon under the TiC formation. As a result, boron partially (by one-third) substituted carbon in the TiC lattice turning it into the carboboride Ti(C,B) with a stoichiometric Ti content (creating the “core” of the duplex particle (Fig. 6a)). The appearance of the “core” resulted in Ti-depletion of the surrounding melt where contents of other alloying elements were still rather high (Fig. 6b). In this area, W, Mo, and V started participating (together with Ti) in the particle formation thus promoting the TiC cubic lattice constructing under the deficiency of Ti atoms. As a result, around the Ti(C,B) “core”, the $(\text{Ti,W,Mo,V})(\text{C,B})$ “shell” appeared, the outer contours of which generally repeat the contours of the “core”. The “shell” grew until the neighboring areas were extremely depleted by Ti, W, Mo, and V (Fig. 6c) which was the termination of the particle formation. It is noteworthy that chromium practically did not contribute to this process despite its high content in the alloy (10 wt.%). This is explained by the lower affinity of chromium for carbon and boron, compared with the above elements [24, 25].

As to the uniform carboborides, they evidently appeared in the melt where the Ti concentration was not sufficient for Ti(C,B) crystallization. Here, Ti, W, Mo, and V act together from the very beginning to build the $(\text{Ti,W,Mo,V})(\text{C,B})$ compound that results in their uniform distribution within the particle. Although here too, titanium plays the key role predetermining the lattice type which is similar to Ti(C,B) . According to the XRD pattern [21], both (duplex and uniform) Ti-rich compounds had the same XRD response performing the diffraction maxima characteristic for the TiC carbide with a cubic lattice of NaCl type. This is also confirmed by the TEM investigation of the duplex inclusion which revealed the TiC-like crystal structure of the “shell” (Fig. 5c). The duplex nature of Ti-rich inclusions is the distinctive feature of a multi-component alloying [21, 22] aimed at the competition of the elements to bind with carbon and boron. This leads to the formation of the non-

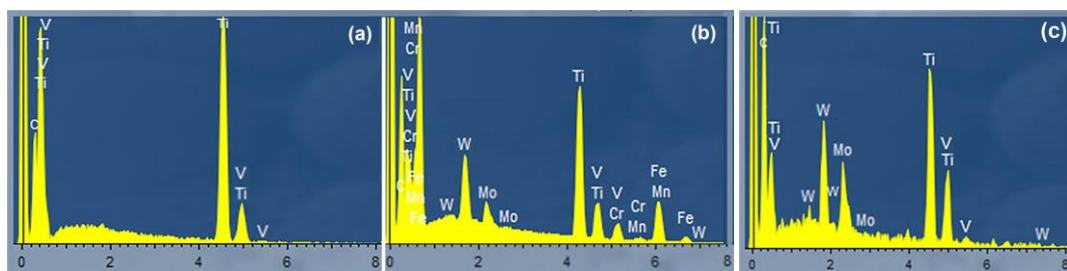


Fig. 4. The EDX spectra of the (a,b) duplex M(C,B) inclusion and (c) uniform M(C,B) inclusion (a – the core and b – the shell).

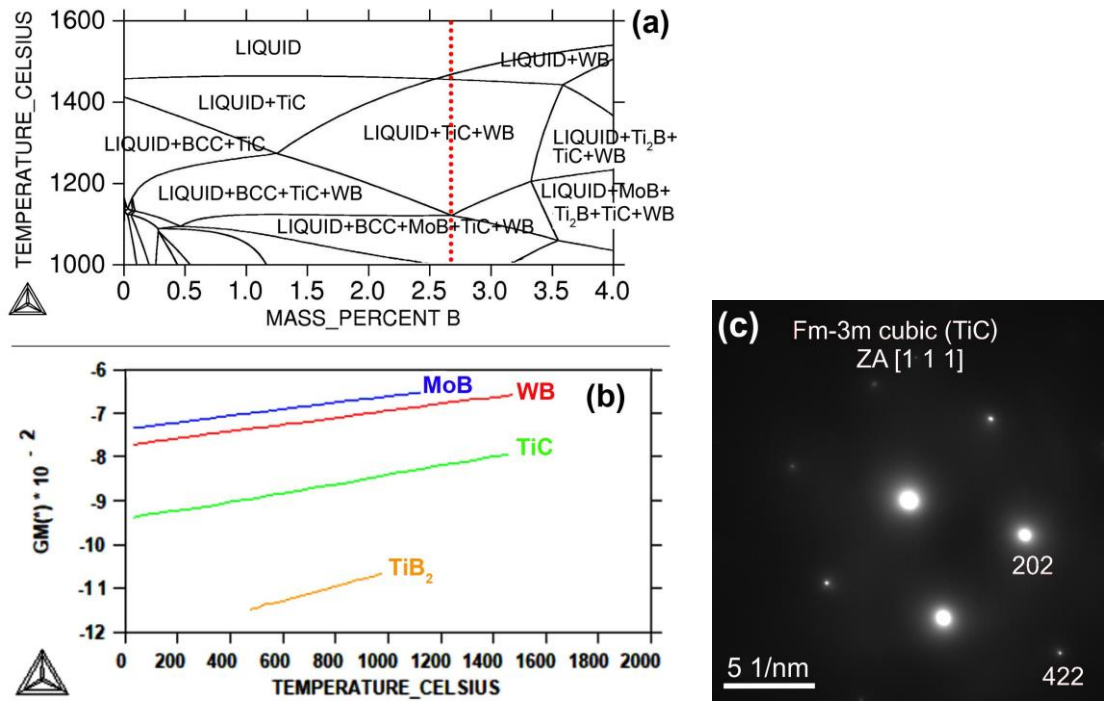


Fig. 5. (a) The calculated pseudo-binary phase diagram of the “M – Boron” system (where M stands for the chemical composition of the alloy studied), (b) the temperature dependence of Gibbs energy for the carbide TiC and borides TiB₂, WB, and MoB, (c) SADE pattern taken from the “shell” of the duplex inclusion. (Figs. (a) and (b) are adopted from [23]).

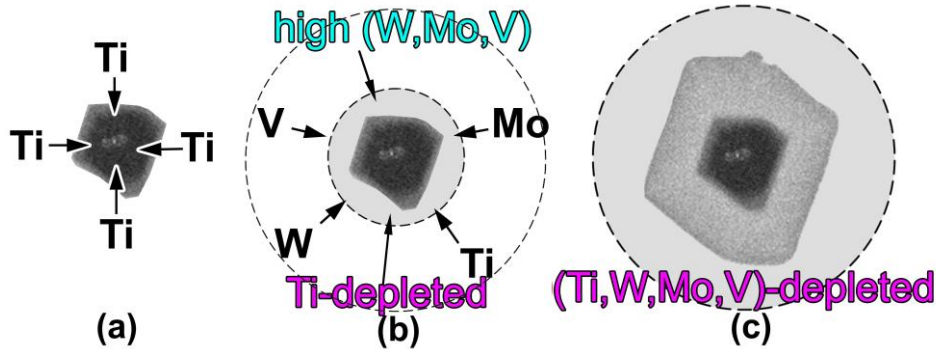


Fig. 6. The mechanism of the duplex M(C,B) formation: (a) the “core” solidification, (b) the start of the “shell” formation, (c) the process completion. (The grey areas are the alloying elements-depleted zones).

stoichiometric phases with a pronounced irregularity in elemental distribution. Apart of the duplex M(C,B) carboboride, this irregularity manifested in duplex morphology of the primary carboborides M₂(B,C)₅ (consisting of a W-rich “core” and W-depleted/Cr-rich “shell”), as well as an apparent segregation of Mo and Fe within the eutectic plates of boroncementite M₃(C,B) [21, 22]. Studying the micromechanical behavior can be the aim of future research in order to fully characterize the duplex nature of a Ti-rich carboboride M(C,B).

Conclusions

It was concluded that adding 2.60 wt.% Ti to the multi-component (wt.%) Fe-0.72C-2.75B-5.05W-5.57Mo-10.35Cr cast alloy results in the formation of Ti-based carboboride M(C,B) of a duplex (“core”/“shell”)

and the uniform morphologies. In the duplex particles, the “core” is a Ti-rich (~75 wt. % Ti) carboboride (Ti_{0.92}V_{0.06}W_{0.01}Fe_{0.01})(C_{0.71}B_{0.29}), while the “shell” is a Ti-depleted (47 wt.% Ti) carboboride (Ti_{0.78}V_{0.11}W_{0.05}Mo_{0.04}Fe_{0.02})(C_{0.77}B_{0.23}). In the uniform particles, the elements are evenly distributed, and the chemical composition is close to the “shell”, containing about 40 wt.% Ti and 30 wt.% (W+Mo+V). In the carboboride M(C,B), the carbon dominated over boron with a B:C (at. %) ratio of 1:2.5 for the “core” and 1:3.3(3.2) – for the “shell” and the uniform inclusions.

Acknowledgements

This research was funded by the Ministry of Education and Science of Ukraine (project No. 0123U101834). V.G. Efremenko, Yu.G. Chabak and V.I. Zurnadzhyy appreciate the support in the framework of the “EU Next Generation EU through the Recovery and

Resilience Plan for Slovakia” under projects No. 09I03-03-V01-00061 and No. 09I03-03-V01-00099 respectively.

Chabak Yu.G. – PhD, Associate Professor, Physics Department;

Golinskyi M.A. – Master student;

Efremenko V.G. – Dr. Sci, Professor, Head of Physics Department;

Zurnadzhy V.I. – PhD, Associate Professor, Physics

Department;

Halfa H. – PhD, Associate Professor, Steel Technology Department;

Efremenko B.V. – PhD, Associate Professor, Bio-Engineering Department;

Tsvetkova E.V. – PhD, Associate Professor, Physics Department;

Dzherenova A.V. –Assistant Professor, Physics Department.

- [1] A. E. Karantzalis, Z. Arni, K. Tsirka, A. Evangelou, A. Lekatou, V. Dracopoulos, *Fabrication of TiC-Reinforced Composites by Vacuum Arc Melting: TiC Mode of Reprecipitation in Different Molten Metals and Alloys*, Journal of Materials Engineering and Performance, 25(8), 12 (2016); <https://doi.org/10.1007/s11665-016-2195-0>.
- [2] Y. Wei, Y. Chen, S. Liang, L. Zhu, Y. Li, L. Jia, *Microstructure and Mechanical Properties of TiC Reinforced TZM Composites Prepared by Spark Plasma Sintering*, International Journal of Refractory Metals and Hard Materials, 116, 13, 2023; <https://doi.org/10.1016/j.jirmhm.2023.106345>.
- [3] S. G. Karnaukh, O. E. Markov, L. I. Aliieva, V. V. Kukhar, *Designing and Researching of the Equipment for Cutting by Breaking of Rolled Stock*, International Journal of Advanced Manufacturing Technology, 109(9-12), 8 (2020); <https://doi.org/10.1007/s00170-020-05824-7>.
- [4] H.O. Pierson, *Handbook of Refractory Carbides and Nitrides: Properties, Characteristics, Processing, and Applications*. (Noyes Publications, Park Ridge, New York, 1996).
- [5] R. N. Jia, T. Q. Tu, K. H. Zheng, Z. B. Jiao, Z. C. Luo, *Abrasive Wear Behavior of TiC-Strengthened Eutectic High Chromium Cast Iron Composites*, Materials Today Communications, 29, 9, (2021); <https://doi.org/10.1016/j.mtcomm.2021.102906>.
- [6] F. V. Guerra-López, A. Bedolla-Jacuinde, C. A. León-Patiño, M. Vázquez-Ramos, *The Effect of Small Additions of Nb and Ti on the Sliding Wear Behavior of a Co-30Cr-5Mo Alloy*, Wear, 522, 18 (2023); <https://doi.org/10.1016/j.wear.2023.204846>.
- [7] Y. Zhou, Y. L. Yang, Da Li, J. Yang, Y. W. Jiang, X. Ren, Q.-X. Yang, *Effect of Titanium Content on Microstructure and Wear Resistance of Fe-Cr-C Hardfacing Layers*, Welding Journal, 91(8), 8 (2012).
- [8] T. V. Loskutova, I. S. Pogrebova, V. G. Khyzhnyak, M. M. Bobina, N. S. Nikitina, *Protective Properties of a New Type Coatings Involving Titanium, Chromium, Aluminum*, Materials Today: Proceedings, 6, 10 (2019); <https://doi.org/10.1016/j.matpr.2018.10.095>.
- [9] Y. Chabak, V. Efremenko, V. Zurnadzhy, V. Puchý, I. Petryshynets, B. Efremenko, V. Fedun, K. Shimizu, I. Bogomol, V. Kulyk, D. Jakubéczyová, *Structural and Tribological Studies of “(TiC+WC)/Hardened Steel” PMMC Coating Deposited by Air Pulsed Plasma*, Metals, 12 (2), 24 (2022); <https://doi.org/10.3390/met12020218>.
- [10] V. V. Kulyk, Z. A. Duriagina, B. D. Vasylyv, *Effects of Yttria Content and Sintering Temperature on the Microstructure and Tendency to Brittle Fracture of Yttria-Stabilized Zirconia*. Archives of Materials Science and Engineering, 109(2), 15 (2021); <https://doi.org/10.5604/01.3001.0015.2625>.
- [11] Y. Zhang, R. Song, Y. Pei, E. Wen, Z. Zhao, *The Formation of TiC-NbC Core-Shell Structure in Hypereutectic High Chromium Cast Iron Leads to Significant Refinement of Primary M₇C₃*, Journal of Alloys and Compounds, 824, 10 (2020); <https://doi.org/10.1016/j.jallcom.2020.153806>.
- [12] X. Wu, J. Xing, H. Fu, X. Zhi, *Effect of Titanium on the Morphology of Primary M₇C₃ Carbides in Hypereutectic High Chromium White Iron*, Materials Science and Engineering: A, 457, (1–2), 6 (2007); <https://doi.org/10.1016/j.msea.2006.12.006>.
- [13] M. O. Vasylyev, S. I. Sidorenko, S. M. Voloshko, T. Ishikawa, *Effect of Low-Energy Inert-Gas Ion Bombardment of the Metal Surface on the Oxygen Adsorption and Oxidation*, Uspehi Fiziki Metallov, 17 (3), 20 (2016); <https://doi.org/10.15407/ufm.17.03.209>.
- [14] A. Bedolla-Jacuinde, R. Correa, J. G. Quezada, C. Maldonado, *Effect of Titanium on the As-Cast Microstructure of a 16% Chromium White Iron*, Materials Science and Engineering: A, 398 (1–2), 12 (2005); <https://doi.org/10.1016/j.msea.2005.03.072>.
- [15] Y. Liu, B. Li, J. Li, L. He, S. Gao, T. G. Nieh, *Effect of Titanium on the Ductilization of Fe-B Alloys with High Boron Content*, Materials Letters, 64 (11), 3 (2010); <https://doi.org/10.1016/j.matlet.2010.03.013>.
- [16] X. Shi, Y. Jiang, R. Zhou, *Effects of Rare Earth, Titanium, and Magnesium Additions on Microstructures and Properties of High-boron Medium-carbon Alloy*, Journal of Iron and Steel Research International, 23, 8 (2016); [https://doi.org/10.1016/S1006-706X\(16\)30180-7](https://doi.org/10.1016/S1006-706X(16)30180-7).
- [17] X. Ren, S. Tang, H. Fu, J. Xing, *Effect of Titanium Modification on Microstructure and Impact Toughness of High-Boron Multi-Component Alloy*, Metals, 11(2), 15 (2021); <https://doi.org/10.3390/met11020193>.
- [18] X. Yao, J. Ji, Y. Lin, Y. Sun, L. Wang, A. He, B. Wang, P. Lu, M. He, X. Zhang, *TMB₂C (TM = Ti, V): 2D Transition Metal Borocarbide Monolayer with Intriguing Electronic, Magnetic and Electrochemical Properties*, Applied Surface Science, 605, 154692 (2022); <https://doi.org/10.1016/j.apsusc.2022.154692>.

- [19] D. Liu, R. Liu, Y. Wei, Y. Ma, K. Zhu, *Microstructure and Wear Properties of Fe–15Cr–2.5Ti–2C–xBwt.% Hardfacing Alloys*, Applied Surface Science, 271, 7 (2013); <https://doi.org/10.1016/j.apsusc.2013.01.169>.
- [20] Y. Zhang, K. Shimizu, X. Yaer, K. Kusumoto, V. G. Efremenko, *Erosive Wear Performance of Heat Treated Multi-Component Cast Iron Containing Cr, V, Mn and Ni Eroded by Alumina Spheres at Elevated Temperatures*, Wear, 390-391, 11 (2017); <https://doi.org/10.1016/j.wear.2017.07.017>.
- [21] Yu. G. Chabak, K. Shimizu, V. G. Efremenko, M. A. Golinskyi, K. Kusumoto, V. I. Zurnadzhy, A. V. Efremenko, *Microstructure and Phase Elemental Distribution in High-Boron Multi-Component Cast Irons*, International Journal of Minerals, Metallurgy, and Materials, 29 (1), 10 (2022); <https://doi.org/10.1007/s12613-020-2135-8>.
- [22] V. G. Efremenko, Yu. G. Chabak, K. Shimizu, M. A. Golinskyi, A. G. Lekatou, I. Petryshynets, B. V. Efremenko, H. Halfa, K. Kusumoto, V. I. Zurnadzhy, *The Novel Hybrid Concept on Designing Advanced Multi-Component Cast Irons: Effect of Boron and Titanium (Thermodynamic Modelling, Microstructure and Mechanical Property Evaluation)*, Materials Characterization, 197, 112691, (2023); <https://doi.org/10.1016/j.matchar.2023.112691>.
- [23] Yu. G. Chabak, M. A. Golinskyi, V. G. Efremenko, K. Shimizu, H. Halfa, V. I. Zurnadzhy, B. V. Efremenko, T.M. Kovbasiuk, *Phase Constituents Modeling in Hybrid Multi-Component High-Boron Alloy*, Physics and Chemistry of Solid State, 23(4), 6 (2022); <https://doi.org/10.15330/pcss.23.4.714-719>.
- [24] O. V. Sukhova, V. A. Polonsky, *Structure and Corrosion of Quasicrystalline Cast Al–Co–Ni and Al–Fe–Ni Alloys in Aqueous NaCl Solution*, East European Journal of Physics, 3, 6 (2020); <https://doi.org/10.26565/2312-4334-2020-3-01>.
- [25] Yu. G. Chabak, V. G. Efremenko, *Change of Secondary-Carbides' Nanostate in 14.5% Cr Cast Iron at High-Temperature Heating*, Metallofizika i Noveishie Tekhnologii, 34, 16 (2012).

Ю.Г. Чабак^{1,2}, М.А. Голинський¹, В.Г. Єфременко^{1,2}, Х. Халфа³, В.І. Зурнаджи^{1,2},
Б.В. Єфременко¹, О.В. Цветкова¹, А.В. Джеренова¹

Збагачені на титан карбобориди в мультикомпонентному високобористому сплаві: розподіл хімічних елементів та механізм формування

¹Приазовський державний технічний університет, Маріуполь, Україна, vgefremenko@gmail.com

²Інститут матеріалознавства Словацької Академії наук, Кошице, Словаччина

³Центральний інститут металургійних досліджень і розробок, Елтеббін, Хелван, Каір, Єгипет

У статті наведено результати дослідження морфології, хімічного складу і розподілу хімічних елементів у збагаченому на титан карбобориді М(С,В), присутньому в мультикомпонентному сплаві (мас.%) Fe-0,72C-2,75B-5,05W-5,57Mo-10,35Cr-2,60Ti. Дослідження виконано із застосуванням методів оптичної та скануючої/трансмісійної електронної мікроскопії, а також енергодисперсійної рентгенівської спектроскопії. Встановлено, що карбоборид М(С,В) знаходиться у структурі у вигляді дисперсних полігональних часток середнім розміром 0,5-7,3 мкм із різною морфологією: «дуплексною» та «однорідною». Дуплексні включення мають збагачене на титан (75 мас. %) «ядро» (Ti(С,В)) та збіднену на титан (47 мас. %) «оболонку» ((Ti,W,Mo),V)(С,В)). Однорідні включення характеризуються рівномірним розподілом елементів; за хімічним складом вони близькі до «оболонки» дуплексних часток. Співвідношення В:С (ат.%) для «ядра», «оболонки» та однорідного включення становить 1:2,5, 1:3,3 і 1:3,2, відповідно. Представлено хімічні формули дуплексних та однорідних М(С,В) включень та запропоновано механізм їх утворення.

Ключові слова: мультикомпонентний чавун, мікроструктура, енергодисперсійний аналіз, карбоборид титану, дуплексні включення.